The Performance of a Lensless Fibre-Deployed Low Coherence Interferometer for In-Situ Measurements

T. Hovell, R. S. Matharu, L. Justham, J. Petzing, P. Kinnell
Loughborough University, United Kingdom

Abstract

The need for increased geometric complexity and accuracy in manufactured parts is being industrially driven by sectors such as automotive, aerospace, medical, and energy generation. It is important to not only have traceable measurement systems in place for component geometry and tolerance conformance verification, but also to aid in the control of the material removal process in real-time on machine.
Low Coherence Interferometry (LCI) has been developed and primarily used in the biomedical imaging domain for the past 20 years as Optical Coherence Tomography (OCT). During this period, it has been shown to be a powerful imaging modality with the ability to operate down to micrometre resolution for depth measurements in non-ideal environments. However, literature defining the effectiveness of lensless LCI/OCT systems operating outside of the biomedical domain is more sparse. Furthermore, the impact of system component choice on key output parameters has not been considered.
In this work, the characterisation of a lensless, fibre deployed LCI system in a common path configuration is performed whilst varying system components. Geometric measurements are demonstrated both in air and in water, with analysis of the impact of system design and componentry on output performance metrics. Relative and absolute traceability of results are produced from calibration grade gauge blocks and Renishaw XL-80 calibration experiments to determine and underpin metrological statements of operating characteristics of the system.

1 Introduction

Industrial demands for one-off customised production of components in sectors such as automotive, aerospace, medical and energy generation has led to the requirement for improved manufacturing process control, so processes are able to adapt to provide the required product geometry and surface roughness [1]. This type of process control is only possible through the incorporation of a traceable measurement device during the manufacturing process to provide real-time process feedback for tool inputs. Therefore, new compact and robust sensors that can be easily integrated within the process are required. Fibre-based sensors are of particular interest as they are extremely compact in nature and are inherently robust to many harsh operating conditions.
Low coherence interferometry (LCI) has been shown to be a useful tool for absolute ranging and tomographic measurements in optical fibre defect detection and biomedical applications [2, 3]. LCI has also been able to provide

measurements with resolutions of up to 1 μm [4] in real-time with high frame rates [5], with the added benefit of full-fibre deployed capability giving an extremely low sensor footprint. Although some exploration into the application of this technology in an industrial environment for metrology usage has been completed, such as in the silicon wafer industry [6] and for analysing artwork [7], work on ranging measurements for metallic objects remains very scarce [8, 9].
The potential benefit of LCI is that with relatively inexpensive optical components that are readily available an instrument can be built capable of performing useful measurements making it highly accessible. This makes it ideal for integration into manufacturing procedures, providing in-process measurements. However, there are a range of component choices required when it comes to building the final system, and therefore it is important to understand the impact that the specification of each component has on key system parameters: resolution, precision, range, accuracy and cost. The work presented here describes a common-path, Fourier domain LCI system for the measurement of metallic objects to determine stand-off distance and step-height variation along a measured path, and the impact of varying the systems spectrometer on functional parameters of the measured output from the system. Measurements have been performed in air and water media, to explore the potential of both spectrometers for operating within a simulated manufacturing environment.

2 Background theory

LCI is a non-contact optical sensing technique which has been used for absolute ranging of fibre optic cables termed ‘optical coherence domain reflectometry (OCDR)’ [2], in medical diagnostic applications for tomographic measurements of tissues, and in ophthalmology termed ‘optical coherence tomography (OCT)’ [3]. This research follows on from the developments made in these mentioned fields using an un-lensed, common-path, Fourier domain-based implementation of an LCI system, also referred as spectral domain system. In this work, a broadband light source is used to illuminate a Michelson interferometer, in this system a common-path approach has been taken whereby the reference and object signal share the same optical path. The reference is achieved from the backreflected light at the interface of the fibre and medium and the object signal from backreflected light from the item under inspection. These signals are recombined at the spectrometer to form a modulated interference signal that is dispersed onto a charge coupled device (CCD) array to measure the cross-spectral density.
The spectrometers used in this paper are both using a Czerny-Turner configuration as can be seen in Figure 1, this design makes use of wavelength dependent diffraction, whereby input light is collimated and directed towards a diffraction grating, that separates the wavelength components reflecting them in slightly different directions. The optics then focus the spectra onto the CCD array. Within the spectrometer the three primary variable components that will impact on the performance of the spectrometer are input slit size; diffraction grating groove density and blazed wavelength, and the CCD specifications. Interdependencies between components means that trade-offs between system performance parameters will be required, for this reason it is important to

understand the application and operational requirements of the sensor to ensure appropriate spectrometer specification.
The interferogram data is generated by instrumentation constrained by real-world limitations and in the case of Fourier domain LCI, it is obtained through a sampling operation for rapid digital signal computation of its inverse Fourier transform. This relates to a trade-off between axial resolution and imaging depth due to their inverse relationship, given by equation 1:

$$\Delta z = \left(\frac{\lambda_0^2}{4}\right)\left(\frac{N_S}{\Delta\lambda}\right) \quad (1)$$

Where N_S is the number of pixels for which the light sources spectrum at full-width at half-maximum $\Delta\lambda$ is sampled across. Here, λ_0 denotes the light source centre frequency, hence $\lambda_0^2/\Delta\lambda$ determines the axial resolution δ_Z. Therefore, maximum imaging depth without aliasing can be increased through a decrease in the axial resolution δ_Z or by an increase in the spectral sampling number N_S [10]. The performance of a Fourier-domain base LCI system is directly dependent on the design of an optimum spectrometer. The specification of both spectrometers used in this paper are shown in Table 1.

Table 1: Spectrometer component specifications

	Ocean Optics Maya 2000 Pro	Thorlabs CCS175
Detector	Hamamatsu S11510-1106 with VIS window	Toshiba TCD1304DG
CCD Pixel number	2,048 × 64	3,648 × 1
Quantum efficiency (%) at λ = 853 nm ± 58 nm	80 to 67	44 to 19
Dynamic range	50,000	300
Resolution (px/nm)	~ 2.5	~ 6
Wavelength range (nm)	749 – 923	500 – 1,000
Average resolution (nm)	0.21	0.6
Diffraction grating	1,200 lines/mm, 750 nm Blaze	830 lines/mm, 800 nm Blaze
Slit (width μm × height mm)	25 × 1	20 × 1.2
Read speed (scans/sec)	138	200
Max operating range (mm) calculated from Eq. 1	2.14	1.33
Cost ratio	3.2	1

Slit size
The opening size that allows light into the spectrometer is inversely related to optical resolution of the system, with small sizes limiting light input to light rays which are highly paraxial to the optical axis. However, reducing slit width also decreases the signal strength.

Diffraction grating
Increasing groove density on the diffraction grating will increase resolution but also reduce the spectral range of the spectrometer and acquired signal strength if other elements remain the same. Additionally, the blazed grating wavelength should be at the centre frequency of the broadband source used to ensure maximum efficiency, wavelengths outside the region of best efficiency will appear to have a lower intensity as seen by the detector.
Charge-coupled detector (CCD)
The CCD measures the amount of light entering the system at each wavelength, this acts as a sampling device for the modulated interference spectrum. Hence, array specification has a large impact on system performance. Features such as, pixel number, size and pixel spacing is hugely important for determining the maximum operation range of the spectrometer and the resolution due to the sampling of the signal. Quantum efficiency of the spectrometer specifies how efficiently photons hitting the CCD array are converted to a charge, with quantum efficiency of a sensor not remaining uniform across the operating spectrum. Dynamic range is a measure of the intensity resolution of a spectrometer, determined by the maximum signal before saturation over the minimum signal, where minimum signal equals the baseline noise.

3 Experimental procedure

The system setup used to calibrate the spectrometer readings is shown in Figure 1, this consists of a super-luminescent diode (EXS210068-01, Beratron GmbH), with a 3-dB bandwidth of 58 nm, central wavelength of 853 nm and an emitting power of 5.14 mW at 160 mA. A single mode fibre coupler with a splitting ratio of 50:50 was used for the beam splitting and coupling, with only one branch of signal output being used as the common-path for the signal and reference. The system is un-lensed with the bare cleaved fibre having a numerical aperture of 0.13, resulting in confocal parameter of 83.51 μm and $1/e^2$ transverse resolution of 5 μm.
In order to calibrate the system a flat mirrored sample surface was translated vertically using a stepper driven translation stage (Zaber Technologies: X-LSM025A) whilst being simultaneously measured by both a Renishaw XL-80 interferometer (accuracy assured to ± 0.5 ppm) to act as a traceable reference measurement for the LCI system as shown in Figure 1. This allows for a relationship between LCI sensor measurement and spatial depth to be obtained. The sample was translated in steps of 10 μm for a total distance of either 1,000 μm or 500 μm depending on the spectrometer used. The difference in translated distance is due to component specification differences between the Thorlabs and Ocean Optics spectrometers relating to a different achievable operating range, as calculated in equation 1, and given in Table 1. This calibration experiment was completed four times in air and water for both spectrometers with the data displayed showing the mean value of the results.

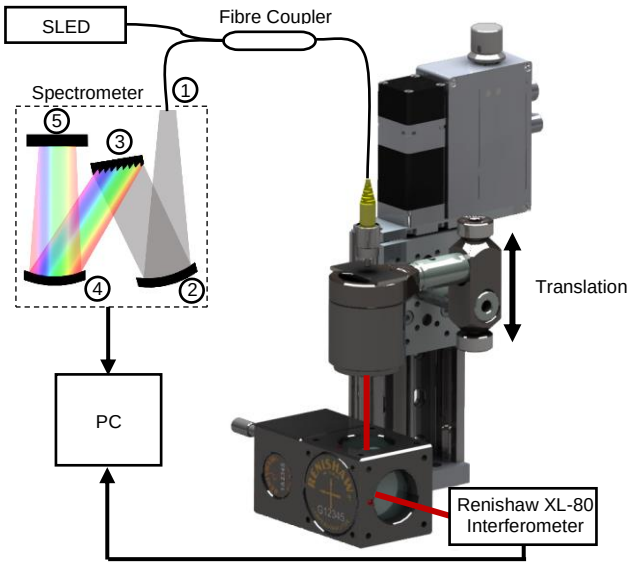

Figure 1: Calibration experimental setup showing Czerny-Turner spectrometer design: 1) Fixed entrance slit, 2) Collimating mirror, 3) Diffraction grating, 4) Focussing mirror, 5) Charge-coupled device (CCD)

Measurements across calibration grade tungsten carbide gauge blocks from Opus of varying heights (8 µm and 6 µm step heights) wrung onto a flat mirror surface were also performed in air and submerged in water. Lateral translation was completed using a set of 3-axis stepper driven stages, (Newport: MFA-PPD) in steps of 25 µm over a translational length of 8.85 mm. The measurements were performed with an initial sample stand-off distance from the fibre tip of ~78 µm and ~157 µm for the Thorlabs and Ocean Optics spectrometers respectively, stand-off difference due to location being selected on peak centre frequency. Measurements were repeated 50 times for each step height and the data displayed is the mean obtained value and standard deviation of measurements.

4 Results for calibration measurements

Figure 2 shows the signal to noise ratio (SNR) of the captured signal during the calibration experiments, from the Thorlabs and Ocean Optics spectrometers as a function of sample distance from the fibre tip, for both air and water media. The reduction in sensitivity with optical path difference in Fourier Domain LCI can be understood as the decreasing visibility of higher fringe frequencies corresponding to large sample depths. This is due to a sampling of the signal occurring at the CCD leading to hardware limitations at larger optical path differences where high frequencies will occur. The achieved resolvable range of the system for both Thorlabs and Ocean Optics spectrometer is less than half that of their calculated maximum possible values before aliasing would occur. This may potentially be due to the system operating with an un-lensed bare fibre thus large amount of dispersion occurring, reducing the amount of back-reflected light being coupled into the fibre to act as the sample signal, and hence reducing

the acquired signal strength. The Ocean Optics spectrometer demonstrates greater SNR over the Thorlabs for both media of operation, this may potentially be due to the difference in quantum efficiency of the CCD over the operating wavelengths of the signal giving a reduced SNR and operable range in the Thorlabs spectrometer. It can be seen for both spectrometers that changing operating media from air to water leads to SNR reduction offset, this is due to the increased refractive index dispersing light at a greater rate than air, and some absorption of light both reducing the backreflected light from the sample into the fibre.

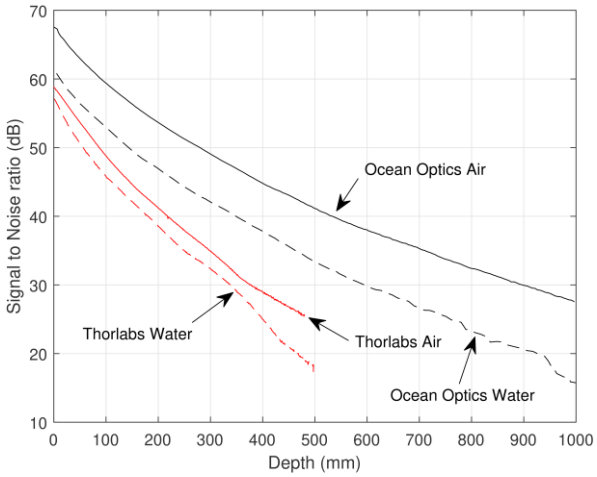

Figure 2: Signal to Noise ratio as a function of depth for Thorlabs and Ocean Optics spectrometers for both water and air

Figure 3 shows the results from the calibration experiments performed with the Ocean optics and Thorlabs spectrometers, using the Renishaw XL-80 to relate the frequency shift of the auto-correlation function frequency extracted from the interferogram of the LCI system and spatial distance.

From Figure 3 transitioning from air to water is seen to provide an offset and reduction in LCI measurement sensitivity, this is due to the increase in refractive index leading to longer signal path lengths relating to an apparent increase in OPD for the same sample offset from the fibre-tip.

The Thorlabs spectrometer is shown to be approximately half as sensitive as the Ocean Optics, only able to measure up to ~500 μm for the same frequency variation as the Ocean Optics which achieves ~1,000 μm. This is due to the difference in resolution with the Thorlabs offering ~6 px/nm against the Ocean Optics giving ~2.5 px/nm, producing greater sensitivity to signal fluctuation. This also means that the Thorlabs spectrometer will have a lower range of operation due to reduced signal sampling coupled with Nyquist theory requirement for a sampling rate of at least two times that of the sampled signal. Hence signal washout will occur at lower optical path differences.

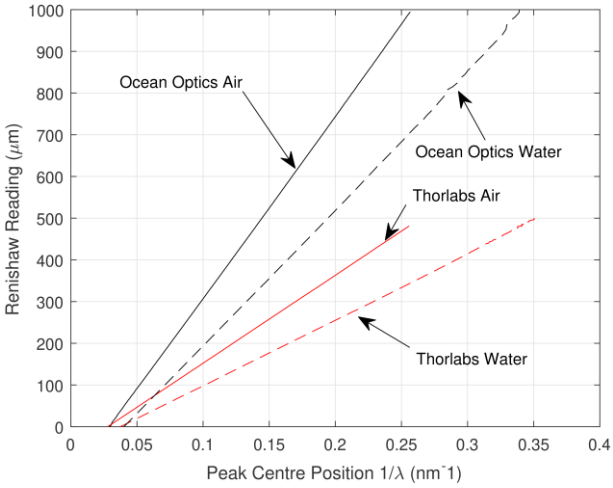

Figure 3: Comparison of calibration data of auto-correlation peak value and absolute depth (Renishaw reading) for Thorlabs and Ocean Optics spectrometers in air and water

Figure 4 shows the residual error between a second order polynomial fit of the calibration data to the absolute value obtained from the Renishaw XL-80. This discrepancy between actual and calculated will show as a residual error in the measurement with the size of the error depending on the operating region of the sensor. Fluctuation in residual error occurs more frequently with the Thorlabs spectrometer as well as having a larger overall error amplitude when compared against the Ocean Optics across it's respective operating range. This may be due to the resolvability of the FFT peak acquired leading to variation in data.

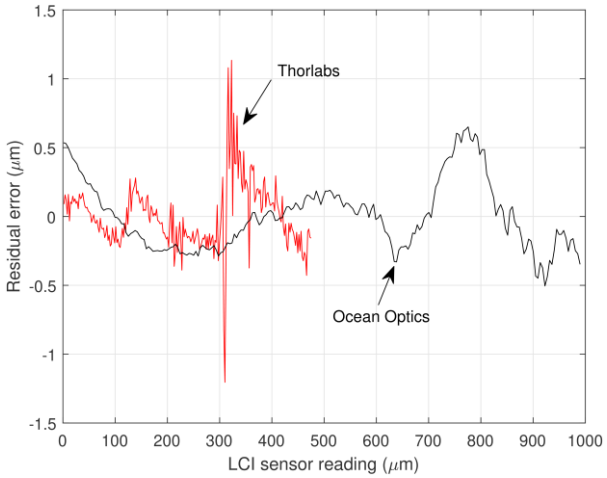

Figure 4: Residual errors for calibration 2nd order polynomial curve fit for Thorlabs and Ocean optics spectrometers

5 Results for slip gauge measurements

In addition to calibration experiments, measurement of 8 μm and 6 μm step heights in air and water was also performed with both spectrometers to demonstrate practical usage for analysis of metallic components. Table 2 contains the results from the experiments and shows for both spectrometers a reduction in performance going from operating in air to water in terms of accuracy and precision, despite accounting for the refractive index change. This decrement in performance is thought to be due to increased dispersion leading to a weaker returned sample signal with more signal noise present and an increase in integrated pathlengths. Except for the 8 μm measurement in water the Ocean Optics demonstrates better performance than the Thorlabs in terms of measurement accuracy and precision across the 50 repeated lateral measurements. From Table 1 there is a ~3.2 to 1 cost ratio between the Ocean Optics and Thorlabs spectrometers respectively, demonstrating on cost the potential viability of a lower cost spectrometer dependent on operational requirements such as detection depth and accuracy.

Table 2: Step height measurements using both Thorlabs and Ocean Optics spectrometers, for measurement in air and in water.

Nominal (μm)*	Medium	Measured Depth Values (μm)			
		Thorlabs	Abs Dev	Ocean Optics	Abs Dev
8	Air	8.48 ± 0.09	0.48	8.33 ± 0.04	0.33
	Water	7.48 ± 0.08	-0.52	8.85 ± 0.21	0.85
6	Air	7.11 ± 0.12	1.11	6.22 ± 0.07	0.22
	Water	5.18 ± 0.35	-0.82	5.40 ± 0.28	-0.60

* Error budget for wringing of slip gauges has not been completed at this stage.

6 Conclusion

This work explores the performance impact of varying the spectrometer in an LCI system performing measurements on metallic components. From observing the implementation of the Ocean Optics and Thorlabs spectrometers a clear difference in achieved results is shown due to component specification. The Thorlabs spectrometer gave a lower SNR with optical path difference in the instrument, a reduction in achievable range due to increased sensitivity falloff, and overall lower precision and accuracy compared with the Ocean Optics spectrometer. When performing measurements within an ideal region of operation the spectrometers have both been shown to provide high quality measurements of step heights, demonstrating that with a simplistic relatively low-cost setup, measurements of components of the micrometre scale is possible albeit with uncertainty budget. It is also worth noting that the Thorlabs spectrometer is ~3.2 times cheaper than the Ocean Optics, hence dependent on the application requirements it may be the preferable choice. To conclude the performance of an LCI system is directly dependent on the spectrometer specification, requiring selection to suit application requirements on operating range, achievable axial resolution, and desired SNR.

References

[1] X. Jiang, "Precision surface measurement," *Philosophical Transactions of the Royal Society of London A: Mathematical, Physical and Engineering Sciences,* vol. 370, no. 1973, pp. 4089 - 4114, 2012.

[2] K. Takada, I. Yokohama, K. Chida and J. Noda, "New measurement system for fault location in optical waveguide devices based on an interferometric technique," *Appl Opt,* vol. 26, pp. 1693 - 1608, 1987.

[3] A. Fercher, K. Mengedoht and W. Werner, "Eye-length measurement by interferometry with partially coherent light," *Opt Lett,* vol. 13, pp. 1867 - 1869, 1988.

[4] W. Drexler, U. Morgner, F. Kärtner, C. Pitris, S. Boppart, X. Li, E. Ippen and J. Fujimoto, "In vivo ultrahigh-resoltion optical coherence tomography: Basics and applications," *Opt Lett,* vol. 24, no. 17, pp. 1221 - 1223, 1999.

[5] M. Wojtkowski, "High-speed optical coherence tomography: Basics and applications," *Appl Opt,* vol. 49, no. 16, pp. 30 - 61, 2010.

[6] H. Park and K. Joo, "High-speed combined NIR low-coherence interferometry for wafer metrology," *Opt. Express,* vol. 56, no. 31, pp. 8592 - 8597, 2017.

[7] D. Hinsch, G. Gülker and H. Helmers, "Checkup for aging artwork—Optical tools to monitor," *Optics and Lasers in Engineering,* vol. 45, no. 5, pp. 578 - 588, 2007.

[8] M. Amaral, P. Raele and et.al, "Roughness measurement methodology according to DIN 4768 using optical coherence tomography (OCT)," in *Modeling Aspects in Optical Metrology II*, Munich, 2009.

[9] D. Stifter, "Beyond biomedicine: a review of alternative applications and developments for optical coherence tomography," *Appl. Phys. B,* vol. 88, no. 3, pp. 337 - 357, 2007.

[10] W. Drexler and G. Fujimoto, Optical Coherence Tomography: Technology and Applications, Switzerland: Springer, 2015.